



Cite this: *Chem. Commun.*, 2025, 61, 11786

Received 18th March 2025,  
Accepted 27th June 2025

DOI: 10.1039/d5cc01523e

rsc.li/chemcomm

# An esterase-sensitive persulfide/hydrogen sulfide generating fluorogenic probe enhances antioxidant response†

Bharat S. Choudhary,<sup>a</sup> Akshi Vashistha,<sup>b</sup> Ankan Ghosh,<sup>b</sup> Rachit Agarwal<sup>b</sup> and Harinath Chakrapani<sup>b\*</sup>

Hydrogen sulfide (H<sub>2</sub>S) and sulfane sulfur species such as persulfides and polysulfides protect the cells from oxidative stress and are central to the endogenous antioxidant response. Here, we designed and developed a tool that is cleaved by esterase to generate phenacylthiol, which is an artificial substrate for 3-mercaptopyruvate sulfurtransferase (3-MST) and non-electrophilic lactone as a by-product. The esterase-sensitive persulfide generator enhances H<sub>2</sub>S and sulfane sulfur and protects chondrocytes from the lethality induced by elevated reactive oxygen species (ROS).

Hydrogen sulfide (H<sub>2</sub>S), a gaseous signaling molecule, is responsible for maintaining redox homeostasis in the cells, and is involved in primary metabolism, antibiotic response, and aging, and is a potential therapeutic agent involved in several diseases such as Parkinson's, Alzheimer's, and Osteoarthritis.<sup>1–4</sup> Several physiological effects of H<sub>2</sub>S are mediated *via* protein persulfidation, a post-translational modification of cysteine residues (RSH) to persulfides (RS-SH), which has protective effects against oxidative stress induced by reactive oxygen species (ROS).<sup>4–6</sup> Persulfides (RS-SH) and polysulfides (RS-(S)<sub>n</sub>H) collectively form the sulfane sulfur pool and have emerged as crucial mediators of the oxidative stress response.<sup>7</sup> Persulfides exhibit superior reactivity in scavenging reactive oxygen species (ROS) and mitigating oxidative stress.<sup>8</sup> Hence, to enhance the cellular persulfides, several persulfide-generating probes that are activated by enzymes,<sup>9–13</sup> light,<sup>14–16</sup> ROS,<sup>17–20</sup> and peroxynitrite<sup>21</sup> have been developed (Fig. 1a). Several of the aforementioned probes have exhibited potential in alleviating oxidative stress. However, many of them produce electrophilic byproducts, which may contribute to the electrophilic stress,<sup>22</sup> and also, the disulfide bonds are susceptible to reaction with thiols.

Persulfides are biosynthesized by the cystathionine-β-synthase (CBS),<sup>8</sup> cystathionine γ-lyase (CSE),<sup>23</sup> cysteinyl-tRNA synthetases (CARS),<sup>24</sup> and 3-mercaptopyruvate sulfur transferase (3-MST)<sup>25,26</sup> (Fig. 1a). We considered 3-MST, an endogenous enzyme that generates persulfides and H<sub>2</sub>S (Fig. 1b).<sup>25,27–29</sup> 3-MST utilizes 3-mercaptopyruvate (3-MP) as the natural substrate and accepts the sulfur from it to form a transient persulfide intermediate in its active site cysteine and an enolate of pyruvate as the byproduct.<sup>30</sup> The sulfur from the persulfide intermediate can be transferred to thiols or proteins and produces H<sub>2</sub>S under reducing conditions.<sup>31</sup> Recently, we developed phenacyl thiol as an artificial substrate for 3-MST and found that it efficiently produces persulfide and H<sub>2</sub>S in the presence of the enzyme (Fig. 1b).<sup>32–34</sup>

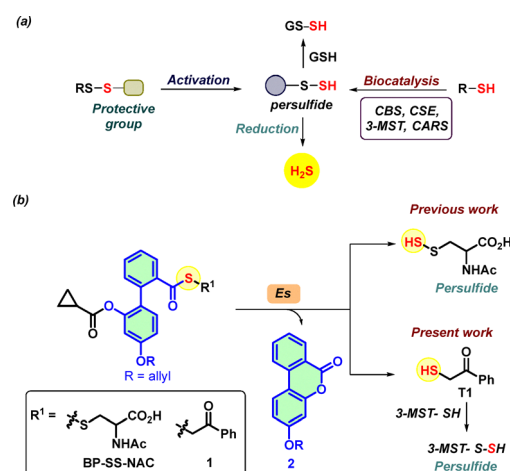


Fig. 1 (a) Methods of persulfide generation via enzymatic or persulfide generating probes, sulfur transfer to GSH, and generation of H<sub>2</sub>S. (b) Reported biphenyl-based persulfide generator in the presence of esterase (Es) generates persulfide and non-electrophilic lactone **2** as a by-product. Based on a similar system, compound **1** generates thiol **T1**, which reacts with 3-MST to generate a persulfide. Previously, phenacyl thioacetate (**AS**) (see ESI,† Scheme S1) was shown to generate **T1** in the presence of esterase.<sup>32</sup>

<sup>a</sup> Department of Chemistry, Indian Institute of Science Education and Research Pune, Pune 411 008, Maharashtra, India. E-mail: harinath@iiserpune.ac.in

<sup>b</sup> Department of Bioengineering, Indian Institute of Science, Bengaluru 560 012, Karnataka, India

† Electronic supplementary information (ESI) available. See DOI: <https://doi.org/10.1039/d5cc01523e>



Our lab also developed a biphenyl-based esterase-sensitive persulfide-generating probe **BP-SS-NAC** that generates persulfide along with a non-electrophilic lactone **2** as a by-product (Fig. 1b).<sup>35</sup> By leveraging the biphenyl scaffold, here, we developed an esterase-sensitive compound that generates phenacyl thiol (**T1**, Fig. 1b). Here, we report results of this compound to generate persulfide and H<sub>2</sub>S in the presence of 3-MST, and protect cells from oxidative stress in a chondrocyte model.

Compound **3** was synthesized following a reported protocol.<sup>35</sup> Compound **3** was reacted with freshly prepared phenacyl thiol (**T1**) in the presence of DCC and DMAP to afford the biphenyl-based esterase-sensitive 3-MST artificial substrate **1** in 20% yield (Scheme 1).

First, to understand if **1** was stable in pH 7.4 buffer, HPLC analysis was carried out. The thioester was found to be stable over 120 min (see ESI,† Fig. S1). In the presence of esterase, as expected, compound **1** produced lactone **2** and **T1** (Fig. 2A). Upon treatment of **1** with esterase, we observed the complete disappearance of **1** (RT 16.7 min) within 60 min, along with the formation of **2** (RT 14.9 min) and **T1** (RT 10.0 min) (Fig. 2B and see ESI,† Fig. S2). HPLC analysis revealed the quantitative formation of **2** and thiol **T1** (Fig. 2C and see ESI,† Fig. S2). In the case of the persulfide analogue **BP-SS-NAC** that we previously reported, the persulfide bond is susceptible to cleavage and thiol exchange, and the perthioester itself was cleaved by Es, leading to a diminished yield of the lactone.<sup>35</sup> Hence, the thioester **1** has advantages in this regard since we find that the yield of the lactone is nearly quantitative.

Since lactone **2** is fluorescent, it can be monitored using fluorescence-based experiments (limit of detection (LOD)  $\approx$  0.3  $\mu$ M, see ESI,† Fig. S3). The compound **1** was itself non-fluorescent, but the addition of Es (1 U mL<sup>-1</sup>) led to a significant increase in fluorescence intensity attributable to the formation of **2** ( $\lambda_{\text{ex}}$  = 320 nm;  $\lambda_{\text{em}}$  = 432 nm) after incubation for 1 h in pH 7.4 buffer (see ESI,† Fig. S4A). Furthermore, a dose-dependent increase in fluorescence was seen during 1 h (see ESI,† Fig. S4B). Curve fitting for the formation of **2** to a first-order exponential equation yielded rate constants ranging from 0.10 to 0.15 min<sup>-1</sup>. The yield of **2** when **1** with Es for 1 h was nearly quantitative, as determined by a fluorescence experiment (see ESI,† Fig. S5). Pre-treatment with PMSF (phenylmethanesulfonyl fluoride), an inhibitor of esterase,<sup>36</sup> resulted in a diminished yield of **2** (see ESI,† Fig. S5). We evaluated the cleavage of compound **1** under cell culture conditions using human chondrocyte C28/I2 cells and observed that **1** was cleaved in whole cells or cell lysates, resulting in a fluorescence signal corresponding to the formation of **2** (see ESI,† Fig. S6 and S7).

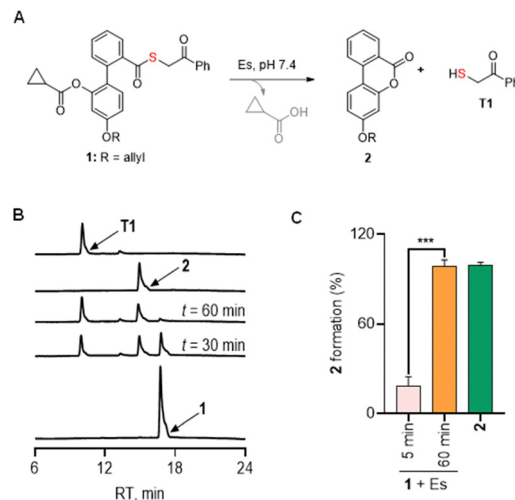
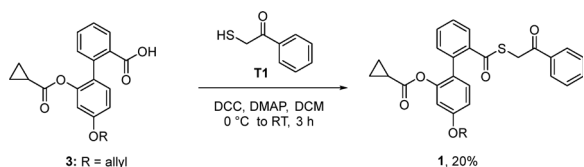


Fig. 2 (A) Compound **1** in the presence of Es is expected to produce lactone **2** and phenacyl thiol **T1** in pH 7.4 buffer at 37 °C. (B) Representative HPLC traces for decomposition of **1** (25  $\mu$ M) and formation of **2** and **T1** in the presence of Es (1 U mL<sup>-1</sup>) (Abs = 250 nm) over 60 min. (C) Area under the curve (AUC) for the peak corresponding to the formation of **2** from **1** as monitored by HPLC. Statistical significance for B and C was carried out using one-way ANOVA (\*\*\*)  $p \leq 0.001$ .

Imaging using confocal microscopy in MEF cells treated with **1** further confirmed the formation of the fluorescent lactone **2** (see ESI,† Fig. S8). Next, the selectivity of **1** for esterase over other biologically relevant species was evaluated, and no significant increase in fluorescence intensity was seen except when **1** was treated with esterase (see ESI,† Fig. S9). Overall, these results supported that **1** underwent lactonization to produce **2** and thiol **T1** following esterase-mediated cleavage.

Next, compound **1** was tested for its ability to generate 3-MST persulfide in the presence of Es and 3-MST, and the sulfur transfer to a small molecule thiol using two independent assays was studied (Fig. 3A). Sulfane sulfur detection was carried out using a well-established fluorogenic probe, SSP-2 (see ESI,† Scheme S2).<sup>37</sup> When the reaction mixture of **1** + Es + 3-MST was incubated with the SSP-2, a significant increase in fluorescence intensity ( $\lambda_{\text{ex}}$  = 482 nm;  $\lambda_{\text{em}}$  = 518 nm), corresponding to the generation of sulfane sulfur. As DTT is known to cleave persulfides, pre-treatment with DTT followed by SSP-2, a reduction in the fluorescence signal was observed (Fig. 3B). The protein persulfide 3-MST-S-S- is known to transfer the sulfhydryl group to the small molecule thiol acceptor such as GSH. A standard LC/MS assay was conducted using an established **HPE-IAM** electrophile as a persulfide trapping agent (see ESI,† Scheme S3).<sup>38</sup> When the reaction mixture of **1** + Es + 3MST was treated with GSH in the presence of **HPE-IAM**, a peak for the formation of the **GSS-HPE-AM** adduct (expected  $m/z$  = 517.1427; observed  $m/z$  = 517.1429) was observed at 7.3 min, indicating the formation of GS-SH (Fig. 3C, D, and see ESI,† Fig. S10). Under these conditions, we also observe **Bis-S-HPE-AM** (expected  $m/z$  = 389.1530; observed  $m/z$  = 389.1537), presumably due to the reaction of **HPE-IAM** with H<sub>2</sub>S formed by the reaction of GS-SH persulfide with GSH (Fig. 3E, and see ESI,† Fig. S11). Under cellular conditions, 3-MST persulfide is reduced



Scheme 1 Synthesis of **1**.



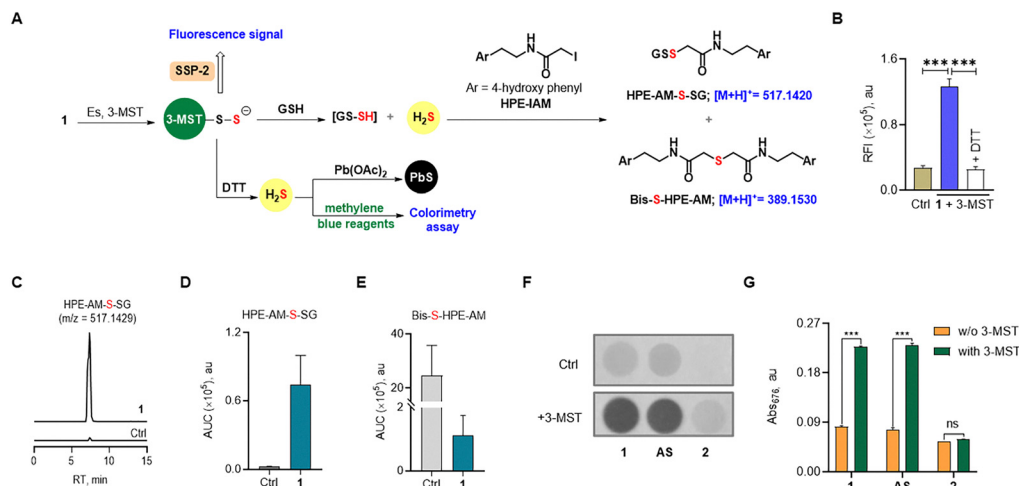


**Fig. 3** (A) Compounds **1** in the presence of Es and 3-MST should produce 3-MST persulfide, and when glutathione is added, the formation of glutathione persulfide (GS-SH) and  $\text{H}_2\text{S}$  is expected. The intermediates of the above are independently detected by various assays. (B) Sulfane sulfur detection with **1** (10  $\mu\text{M}$ ) in the presence of 3-MST (1  $\mu\text{M}$ ), Es (1  $\text{U mL}^{-1}$ ), using SSP-2 (5  $\mu\text{M}$ ) based fluorescent assay. Ctrl: **1** only. +DTT: addition of DTT.  $\lambda_{\text{ex}} = 482 \text{ nm}$  and  $\lambda_{\text{em}} = 518 \text{ nm}$ . (C) LC-MS/MS analyses for persulfide and  $\text{H}_2\text{S}$ : extracted ion chromatogram of HPE-AM-S-SG adduct (expected  $m/z = 517.1427$ ; observed  $m/z = 517.1429$ ) formed upon incubation of **1** (25  $\mu\text{M}$ ) with 3-MST (5  $\mu\text{M}$ ) in the presence of Es (1  $\text{U mL}^{-1}$ ), followed by sequential addition of thiol acceptor (GSH; 1 mM) and electrophilic thiol acceptor (HPE-IAM; 10 mM). Ctrl was prepared by reacting 200  $\mu\text{M}$  GSH, 200  $\mu\text{M}$  DEA/NO (sodium 2-(*N,N*-diethylamino)-diazolene-2-oxide), and 200  $\mu\text{M}$  NaSH at room temperature for 20 min. (D) The area under the curve (AUC) for the peak corresponds to HPE-AM-S-SG. (E) The area under the curve (AUC) for the peak corresponds to Bis-S-HPEAM adduct (expected  $m/z = 389.1530$ ; observed  $m/z = 389.1516$ ). (F)  $\text{H}_2\text{S}$  detection of compounds (**1**, **AS**, and **2**) at 100  $\mu\text{M}$  in the presence of 3-MST (1  $\mu\text{M}$ ), Es (1  $\text{U mL}^{-1}$ ), and DTT (10 mM) for 2 h using lead acetate assay. Ctrl represents only compounds. +3-MST refers to the incubation with 3-MST. (G)  $\text{H}_2\text{S}$  detection of compounds (**1**, **AS**, and **2**) at 100  $\mu\text{M}$  in the presence of 3-MST (1  $\mu\text{M}$ ), Es (1  $\text{U mL}^{-1}$ ), and DTT (10 mM) for 2 h using the methylene blue assay. All data are represented as mean  $\pm$  SD ( $n = 3$ ). Statistical significance for B and G was carried out using One-way ANOVA ( $***p \leq 0.001$ ).

by thioredoxin reductase to produce  $\text{H}_2\text{S}$  and 3-MST.<sup>31</sup> The  $\text{H}_2\text{S}$  formation from compound **1** in the presence of Es, 3-MST, and DTT (a mimic of thioredoxin reductase) was evaluated using two independent assays (Fig. 3A).<sup>32</sup> Firstly, the formation of  $\text{H}_2\text{S}$  from compound **1**, lead acetate assay, was employed (see ESI,† Scheme S4). The addition of an aliquot of the reaction mixture containing **1**, Es, 3-MST, and DTT to lead acetate paper resulted in a dark coloration, indicating the formation of lead sulfide (Fig. 3F and see ESI,† Fig. S12). As expected, positive control **AS** gave a good signal for  $\text{H}_2\text{S}$ , whereas lactone **2** did not produce any  $\text{H}_2\text{S}$  (Fig. 3F and see ESI,† Fig. S12).

Next, we measured  $\text{H}_2\text{S}$  formation using a standard methylene blue (MB) colorimetric assay (see ESI,† Scheme S5); indeed, the results of this assay corroborated with the lead acetate assay (Fig. 3G).

Osteoarthritis (OA) is the most common joint disease and is characterized by a gradual loss of articular cartilage and joint hypertrophy.<sup>39</sup> A study has shown that the  $\text{H}_2\text{S}$  generated from 3-MST protects against joint calcification and severe osteoarthritis.<sup>3</sup> So, enhancing the  $\text{H}_2\text{S}$  and sulfane sulfur in chondrocytes may represent a potential way to treat OA. We first used human chondrocyte C28/I2 cells in culture and found that **1** was well tolerated up to 100  $\mu\text{M}$  after 24 h of incubation (Fig. 4A). Given the central role of oxidative stress in the progression of OA,<sup>40,41</sup> we determined the cytoprotective effects of **1** in C28/I2 cells against oxidative stress induced by a cell-permeable ROS generator (MGR1).<sup>42</sup> Cells were pre-incubated with **1** for 3 h and then exposed to MGR-1 (15  $\mu\text{M}$ ), after which cell metabolic activity was

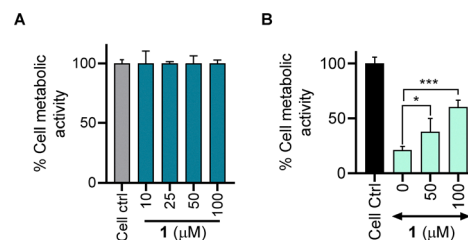


**Fig. 4** Cell metabolic activity assay conducted on C28/I2 cells. (A) Cells treated with varying concentrations of compound **1** for 24 h. (B) Cells treated with varying concentrations of **1** followed by treatment with MGR-1 (15  $\mu\text{M}$ ). All data are presented as mean  $\pm$  SD ( $n = 4/\text{group}$ ). Statistical significance was established relative to MGR-1 using One-way ANOVA ( $*p < 0.033$ ,  $***p \leq 0.001$ ).

assessed. As expected, exposure of cells to MGR-1 resulted in a drastic reduction in cell metabolic activity. However, pre-treatment of cells with **1** demonstrated significant protective effects, rescuing cells from ROS-induced oxidative stress in a concentration-dependent manner (Fig. 4B). This result was also seen with **BP-SS-NAC**, and supports the applicability of the phenacylthiol-based strategy for mitigating oxidative stress.<sup>35</sup>

Next, we utilized micromass cultures derived from the C28/I2 cell line, an *in vitro* model for cartilage,<sup>43</sup> to evaluate the ability of **1** to sustain sGAG production under oxidative stress induced by MGR-1 and found that cells were capable of sustaining sGAG when treated with compound **1** (see ESI,† Fig. S13). Overall, these results suggest that **1** was capable of protecting cells from oxidative stress.



In summary, we report a new persulfide generator that is cleaved by esterase to generate phenacylthiol, an artificial substrate for 3-MST, along with a non-electrophilic and fluorescent by-product. The compound was able to generate lactone quantitatively, and the resulting fluorescence can be useful for use in cellular experiments. The antioxidant property of **1** in chondrocytes serves as a proof-of-principle for this strategy, while further work is needed to characterize precise mechanisms.

Financial assistance for this project was from IISER Pune and ANRF Science and Engineering Research Board (HC, CRG/2023/003892). The manuscript was written with inputs from all authors. BSC, AV, and AG carried out all experiments under the supervision of RA and HC.

## Conflicts of interest

There are no conflicts to declare.

## Data availability

The data supporting this article have been included as part of the ESI.†

## Notes and references

- 1 T. V. Mishanina, M. Libiad and R. Banerjee, *Nat. Chem. Biol.*, 2015, **11**, 457–464.
- 2 M. R. Filipovic, J. Zivanovic, B. Alvarez and R. Banerjee, *Chem. Rev.*, 2018, **118**, 1253–1337.
- 3 S. Nasi, D. Ehrichtiou, A. Chatzianastasiou, N. Nagahara, A. Papapetropoulos, J. Bertrand, G. Cirino, A. So and N. Busso, *Arthritis Res. Ther.*, 2020, **22**, 49.
- 4 A. K. Mustafa, M. M. Gadalla, N. Sen, S. Kim, W. Mu, S. K. Gazi, R. K. Barrow, G. Yang, R. Wang and S. H. Snyder, *Sci. Signaling*, 2009, **2**, ra72.
- 5 C. Yang, N. O. Devarie-Baez, A. Hamsath, X. Fu and M. Xian, *Antioxid. Redox Signaling*, 2020, **33**, 1092–1114.
- 6 H. Kimura, *Br. J. Pharmacol.*, 2020, **177**, 720–733.
- 7 T. Zhang, H. Tsutsuki, K. Ono, T. Akaike and T. Sawa, *J. Clin. Biochem. Nutr.*, 2021, **68**, 5–8.
- 8 T. Ida, T. Sawa, H. Ihara, Y. Tsuchiya, Y. Watanabe, Y. Kumagai, M. Suematsu, H. Motohashi, S. Fujii, T. Matsunaga, M. Yamamoto, K. Ono, N. O. Devarie-Baez, M. Xian, J. M. Fukuto and T. Akaike, *Proc. Natl. Acad. Sci. U. S. A.*, 2014, **111**, 7606–7611.
- 9 Y. Zheng, B. Yu, Z. Li, Z. Yuan, C. L. Organ, R. K. Trivedi, S. Wang, D. J. Lefer and B. Wang, *Angew. Chem., Int. Ed.*, 2017, **56**, 11749–11753.
- 10 Z. Yuan, Y. Zheng, B. Yu, S. Wang, X. Yang and B. Wang, *Org. Lett.*, 2018, **20**, 6364–6367.
- 11 K. M. Dillon, R. J. Carrazzone, Y. Wang, C. R. Powell and J. B. Matson, *ACS Macro Lett.*, 2020, **9**, 606–612.
- 12 K. M. Dillon, H. A. Morrison, C. R. Powell, R. J. Carrazzone, V. M. Ringel-Scaia, E. W. Winckler, R. M. Council-Troche, I. C. Allen and J. B. Matson, *Angew. Chem., Int. Ed.*, 2021, **60**, 6061–6067.
- 13 P. Bora, M. B. Sathian and H. Chakrapani, *Chem. Commun.*, 2022, **58**, 2987–2990.
- 14 A. Chaudhuri, Y. Venkatesh, J. Das, M. Gangopadhyay, T. K. Maiti and N. D. P. Singh, *J. Org. Chem.*, 2019, **84**, 11441–11449.
- 15 A. Chaudhuri, Y. Venkatesh, B. C. Jena, K. K. Behara, M. Mandal and N. D. P. Singh, *Org. Biomol. Chem.*, 2019, **17**, 8800–8805.
- 16 B. Roy, M. Shieh, T. Takata, M. Jung, E. Das, S. Xu, T. Akaike and M. Xian, *J. Am. Chem. Soc.*, 2024, **146**, 30502–30509.
- 17 C. R. Powell, K. M. Dillon, Y. Wang, R. J. Carrazzone and J. B. Matson, *Angew. Chem., Int. Ed.*, 2018, **57**, 6324–6328.
- 18 R. A. Hankins, S. I. Suarez, M. A. Kalk, N. M. Green, M. N. Harty and J. C. Lukesh, *Angew. Chem., Int. Ed.*, 2020, **59**, 22238–22245.
- 19 P. Bora, P. Chauhan, S. Manna and H. Chakrapani, *Org. Lett.*, 2018, **20**, 7916–7920.
- 20 Y. Wang, K. M. Dillon, Z. Li, E. W. Winckler and J. B. Matson, *Angew. Chem., Int. Ed.*, 2020, **59**, 16698–16704.
- 21 Y. Xu, B. Xu, J. Wang, H. Jin, S. Xu, G. Wang and L. Zhen, *Chem. – Eur. J.*, 2022, **28**, e202200540.
- 22 D. C. Thompson, J. A. Thompson, M. Sugumaran and P. Moldéus, *Chem.-Biol. Interact.*, 1993, **86**, 129–162.
- 23 T. Yamanishi and S. Tuboi, *J. Biochem.*, 1981, **89**, 1913–1921.
- 24 T. Akaike, T. Ida, F. Y. Wei, M. Nishida, Y. Kumagai, M. M. Alam, H. Ihara, T. Sawa, T. Matsunaga, S. Kasamatsu, A. Nishimura, M. Morita, K. Tomizawa, A. Nishimura, S. Watanabe, K. Inaba, H. Shima, N. Tanuma, M. Jung, S. Fujii, Y. Watanabe, M. Ohmuraya, P. Nagy, M. Feelsch, J. M. Fukuto and H. Motohashi, *Nat. Commun.*, 2017, **8**, 1177.
- 25 N. Nagahara, T. Yoshii, Y. Abe and T. Matsumura, *J. Biol. Chem.*, 2007, **282**, 1561–1569.
- 26 N. Nagahara, M. Tanaka, Y. Tanaka and T. Ito, *Antioxidants*, 2019, **8**, 116.
- 27 Y. Kimura, S. Koike, N. Shibuya, D. Lefer, Y. Ogasawara and H. Kimura, *Sci. Rep.*, 2017, **7**, 10459.
- 28 B. Pedre and T. P. Dick, *Biol. Chem.*, 2021, **402**, 223–237.
- 29 B. Pedre, D. Talwar, U. Barayeu, D. Schilling, M. Luzarowski, M. Sokolowski, S. Glatt and T. P. Dick, *Nat. Chem. Biol.*, 2023, **19**, 507–517.
- 30 N. Nagahara and T. Nishino, *J. Biol. Chem.*, 1996, **271**, 27395–27401.
- 31 P. K. Yadav, K. Yamada, T. Chiku, M. Koutmos and R. Banerjee, *J. Biol. Chem.*, 2013, **288**, 20002–20013.
- 32 P. Bora, S. Manna, M. A. Nair, R. R. M. Sathe, S. Singh, V. S. Sreyas Adury, K. Gupta, A. Mukherjee, D. K. Saini, S. S. Kamat, A. B. Hazra and H. Chakrapani, *Chem. Sci.*, 2021, **12**, 12939–12949.
- 33 S. Manna, R. Agrawal, T. Yadav, T. A. Kumar, P. Kumari, A. Dalai, S. Kanade, N. Balasubramanian, A. Singh and H. Chakrapani, *Angew. Chem., Int. Ed.*, 2024, **63**, e202411133.
- 34 S. M. Gupta, P. S. Mohite and H. Chakrapani, *Chem. Sci.*, 2025, **16**, 4695–4702.
- 35 B. S. Choudhary, T. A. Kumar, A. Vashishtha, S. Tejasri, A. S. Kumar, R. Agarwal and H. Chakrapani, *Chem. Commun.*, 2024, **60**, 1727–1730.
- 36 P. C. Smith, A. F. McDonagh and L. Z. Benet, *J. Pharmacol. Exp. Ther.*, 1990, **252**, 218–224.
- 37 W. Chen, C. Liu, B. Peng, Y. Zhao, A. Pacheco and M. Xian, *Chem. Sci.*, 2013, **4**, 2892–2896.
- 38 H. A. Hamid, A. Tanaka, T. Ida, A. Nishimura, T. Matsunaga, S. Fujii, M. Morita, T. Sawa, J. M. Fukuto, P. Nagy, R. Tsutsumi, H. Motohashi, H. Ihara and T. Akaike, *Redox Biol.*, 2019, **21**, 101096.
- 39 J. Martel-Pelletier, *Osteoarthr. Cartil.*, 1998, **6**, 374–376.
- 40 M. Y. Ansari, N. Ahmad and T. M. Haqqi, *Biomed. Pharmacother.*, 2020, **129**, 110452.
- 41 L. Liu, P. Luo, M. Yang, J. Wang, W. Hou and P. Xu, *Front. Mol. Biosci.*, 2022, **9**, DOI: [10.3389/fmolb.2022.1001212](https://doi.org/10.3389/fmolb.2022.1001212).
- 42 D. S. Kelkar, G. Ravikumar, N. Mehendale, S. Singh, A. Joshi, A. K. Sharma, A. Mhetre, A. Rajendran, H. Chakrapani and S. S. Kamat, *Nat. Chem. Biol.*, 2019, **15**, 169–178.
- 43 K. V. Greco, A. J. Iqbal, L. Rattazzi, G. Nalesso, N. Moradi-Bidhendi, A. R. Moore, M. B. Goldring, F. Dell'Accio and M. Perretti, *Biochem. Pharmacol.*, 2011, **82**, 1919–1929.

